NUMERICAL STUDY ON FLAME AND EMISSION CHARACTERISTICS OF A SMALL FLUE GAS SELF-CIRCULATION DIESEL BURNER WITH DIFFERENT SPRAY CONE ANGLES

by

Kai XIE [a*], ***Jie ZHANG*** [a], ***Changlin QIN*** [a], ***Xiufeng TAN*** [b], **and** ***Yunjing CUI*** [c]

[a] School of Intelligent Manufacturing, Weifang University of Science and Technology, Weifang, China
[b] Weifang Key Lab of Advanced Light Materials Manufacturing and Forming, Weifang University of Science and Technology, Weifang, China
[c] College of Electromechanical Engineering, China University of Petroleum (East China), Tsingtao, China

Original scientific paper
https://doi.org/10.2298/TSCI201229150X

The problems of long flame and high pollution emissions in low power burners are of wide concern in small heating devices. To solve this problem, a small diesel burner with self-circulation flue gas was designed herein. In order to obtain a deeper scientific understanding of the flame and emission characteristics of the burner with different spray cone angles, a numerical calculation method was used to investigate them. Reasonable flow, heat transfer, and combustion models were selected, and periodic boundary conditions were used to verify the feasibility of the numerical model. The results indicate that the flame length increases with increasing spray cone angle, and then the flame length basically stabilizes at 410 mm. The maximum flame temperature decreases slightly with increasing spray cone angle. Besides this, the NO emission of this small flue gas self-circulation burner decreases with increasing spray cone angle and is as low as 10 ppm at an 80° spray cone angle. In addition, the influence mechanism of the spray cone angle on the flue gas self-circulation ratio was analyzed from the physical aspect of the spray area and the chemical aspect of combustion. This study is of great significance to research on the flame morphology of small flue gas self-circulation burners and the selection of different spray cone angles.

Key words*: spray cone angle, spray flame, NO emission, flame height, re-circulation ratio*

Introduction

Oil burners are widely used in various industrial and civil heating equipment, such as boilers and stoves [1]. At present, the miniaturization of limited heating equipment is increasingly attracting attention, especially in small stoves. A burner with flue gas self-circulation is an effective way to solve the defects of excessive flame length and high NO emissions. In this kind of small burner, the spray cone angle has a vital influence on the flame and emission characteristics.

At present, the international general methods to reduce NO emission mainly include the two-stage combustion method [2], flue gas re-circulation method [3], low oxygen combustion [4], bias combustion technology [5], and non-flame combustion technology [6]. The

* Corresponding authors, e-mails: xiekai@wfust.edu.cn; xiekai199101@163.com

internal structures of burners with graded combustion and bias combustion are complex. Flue gas reversed flow requires a circulating fan, and flameless combustion requires an efficient heat storage device. Flue gas re-circulation combustion technology can be divided into self flue gas re-circulation and fan inlet flue gas re-circulation. Among these, in flue gas self-circulation, the flue gas is made to circulate in the burner by improving the structure of the burner and using the ejecting effect of combustion air. Therefore, for simplicity and economy of small heating devices, flue gas self-circulation combustion technology has gradually attracted the attention of scientists.

Shinomori *et al.* [7] designed a 65 kW oil burner for a small boiler with self-circulating flue gas. The burners control the flue gas reversed flow by varying the size of the flue gas return orifice. The results of particle image velocimetry flow field testing and experimental study showed that the flue gas gradually changed from yellow fire to blue fire with increasing flue gas reversed flow. The volumetric reversed flow ratio of the flue gas in this structure is up to 50%, which can reduce NO emissions from 222-32 mg/m^3 (3% O_2). Xie *et al.* [8] designed a small burner with a flue gas self-circulation structure and studied the effect of different air distribution ratios on the flame length. Xu *et al.* [*9*] conducted detailed experiments and numerical studies on a large flue gas self-circulation burner fueled by coke oven gas and found that NO emissions could be greatly reduced by adjusting and optimizing the operating parameters [10].

Previous researchers have explored the use of fuel nozzles in conventional burners, high powered boilers, and reheating furnaces using theoretical and experimental methods [11, 12]. It was found that the spray cone angle has important effects on flame height, width, temperature, and NO emission [13, 14] because it affects the fuel distribution [15] and atomization state in the initial combustion area [16]. It is generally believed that with decreasing spray cone angle at the same flow rate, the spray penetration distance will increase and the flame height will be greater. Bonefačić *et al.* [17] conducted experimental studies on a 7 MW oil-fired boiler with different spray cone angles and found that a larger spray cone angle in such a large furnace could optimize the spatial distribution of droplets in the outlet area of the burner. San Jose *et al.* [18] conducted experimental research on a low pressure auxiliary air-fluid atomizer under different test conditions and found that the lower the spray cone angle, the greater the combustion efficiency. Amoresano *et al.* [19] investigated combustion evolution by utilizing a high speed camera and the Lagrangian method to determine cone angle fluctuation of the pressure atomizing nozzle. They found that each combustor exhibited its best combustion and heat transfer properties only under specific design conditions, depending on the value of the spray cone angle. This is because the mixing of the two-phases is heavily dependent on the angle of the two flows, including the jet fuel and the oxidized air.

However, these experiments were carried out in a conventional burner or a high powered furnace. There are few studies on small fuel gas self-circulation burners below 40 kW, and there are few reports on the consideration of the spray cone angle in such small burners. However, the spray cone angle has a direct effect on the atomization distribution characteristics of droplets in fuel burners [20], especially in such small burners and confined spaces [21]. Filling the knowledge gap in the aforementioned effect of the spray cone angle of a small flue gas self-circulation burner is also the innovation of this paper. Umyshev *et al.* [22] studied NO emissions for different *V*-shaped jet cone angles using propane as the fuel and found that NO emissions decreased and combustion efficiency increased as the spray cone angle decreased.

In this paper, based on the combustion head structure of the Riello G40 fuel burner, a kind of burner with a flue gas self-circulation structure was developed. In the previous literature, we studied different air distribution ratios and obtained relatively short flames when the central air, swirling air, and secondary air proportions were 35%, 25%, and 40%, respectively. Based on these proportions, the flame length and NO emission characteristics at different spray cone angles (50-90°) were numerically studied in this work.

Model of the flue gas self-circulation burner

Structure of the small flue gas self-circulation burner

The basic structure of the small flue gas re-circulation fuel burner is shown in fig. 1. We added a 35 mm high combustion outer cylinder above the initial flame holder, which was connected by brackets on both sides. A 7.5 mm high annular opening was opened at the bottom of the outer cylinder. In normal combustion, a negative pressure area will form above the flame holder, and the flue gas can then flow back to the combustion cylinder from the opening to form flue gas self-circulation combustion. The specific sizes and internal cross-section are shown in fig. 2.

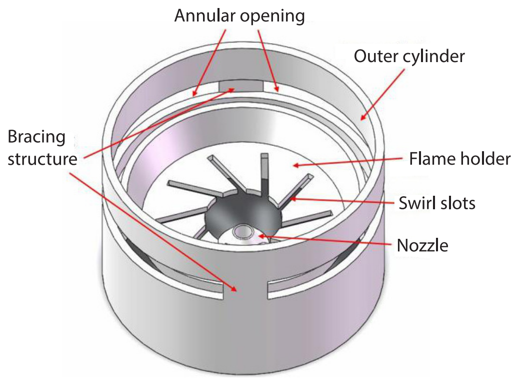

Figure 1. A schematic diagram of the combustion head for a small flue gas self-circulation burner

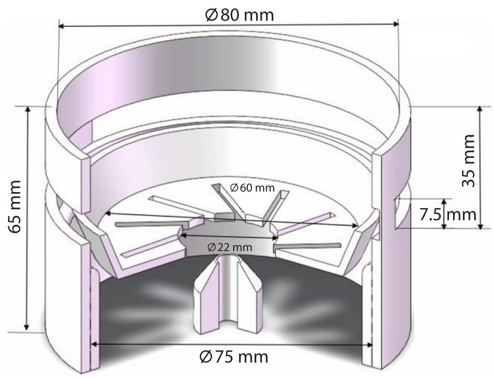

Figure 2. A schematic diagram of the inner section and dimensions of the burner head

The ratio of the flue gas reversed flow at the annular opening to the mass-flow at the outlet is defined as the flue gas self-circulation ratio:

$$\eta_r = \frac{m_r}{m_{\text{out}}} \tag{1}$$

where η_r is the flue gas self-circulation ratio, m_r [kgs^{-1}] – the quantity of reversed flow flue gas, and m_{out} [kgs^{-1}] – the exit mass-flow rate.

Previous studies have shown that although the amount of self-circulating flue gas is mainly affected by the proportions of primary air and secondary air distribution, variation of the spray cone angle also affects the air-flow distribution over the flame plate. We will also analyze this briefly in the discussion of the results.

This paper mainly considers the effect of the spray cone angle on the flame and emission of a low power flue gas self-circulation burner. Figure 3 is a schematic diagram of the spray cone angle. Based on the actual situation, variation of the spray cone angle from 50-90° was mainly considered in the numerical experiments.

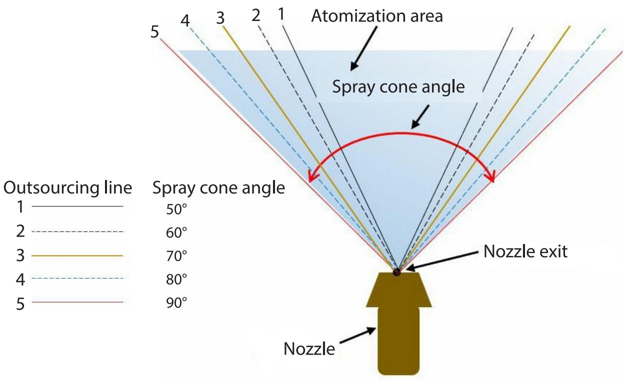

Figure 3. A diagram of the spray cone angle

Computational model and meshing

Due to the symmetry of the combustion head model and the furnace, the calculation cost can be reduced, and the model can be simplified in simulation. Periodic boundary conditions were adopted to simulate only one-fifth of the shape and simplify the nozzle structure at the same time. The total length and diameter of the combustor were 1150 mm and 500 mm, respectively. The flue gas outlet at the top was 250 mm in diameter, and the overhanging length was 150 mm. A schematic diagram of the combustor model size and mesh division is shown in fig. 4.

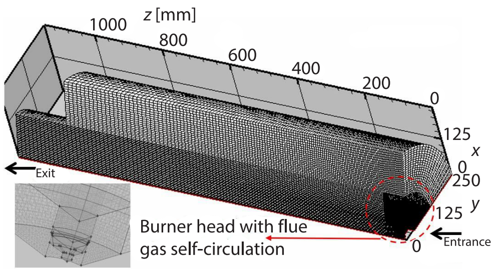

Figure 4. A schematic diagram of the combustor model size and mesh division

The combustion head structure studied in this paper is relatively complex, and even after the model was simplified using periodic boundary conditions, well-integrated grid division could not be achieved. At the same time, considering the grid quality and computational cost, the method of block grid division was adopted for the model, that is, for the regular area of the combustion chamber and combustion cylinder, common structured grid division was adopted, and for irregular areas such as the small flame holder, unstructured grid division was adopted. The mesh of the burner head section was densely processed, while the mesh size of the furnace area away from the combustion area could be slightly larger. The maximum skewness of the grid was controlled below 0.8.

Numerical methods and validation

Fundamental governing equation

The mass conservation equation, namely, the continuity equation, has the differential form of conservation:

$$\frac{\partial \rho}{\partial t}+\frac{\partial}{\partial x_i}(\rho u_i)=0 \tag{2}$$

For the momentum conservation equation of incompressible fluid, namely, the N-S equation, its differential form is shown:

$$\frac{\partial}{\partial t}(\rho u_i)+\frac{\partial}{\partial x_j}(\rho u_i u_j)=\rho f_i-\frac{\partial p}{\partial x_i}+\frac{\partial}{\partial x_j}\left(\mu\frac{\partial u_i}{\partial x_j}\right) \tag{3}$$

where f_i is the mass force on a unit mass of fluid and u_i – the insantaneosus velocity in the *i*-direction.

The component conservation equation, namely, the component diffusion equation, can be simplified for the steady-state conservation equation of component *i* in a multi-component gas:

$$\rho u\frac{\partial Y_i}{\partial x}+\rho v\frac{\partial Y_i}{\partial y}+\rho w\frac{\partial Y_i}{\partial z}=\frac{\partial}{\partial x}\left(\rho D_i\frac{\partial Y_i}{\partial x}\right)+\frac{\partial}{\partial y}\left(\rho D_i\frac{\partial Y_i}{\partial y}\right)+\frac{\partial}{\partial z}\left(\rho D_i\frac{\partial Y_i}{\partial z}\right)-w_i \tag{4}$$

where Y_i is the concentration of component *i*, D_i – the diffusion coefficient of component *i*, and w_i – the formation rate of the net reaction.

In the numerical calculation of the combustion process, radiation, convection, and component diffusion should be considered simultaneously. The energy equation:

$$\begin{aligned}&\frac{\partial(\rho e)}{\partial t}+\nabla(\rho e\mathbf{V})=\rho\dot{q}+\left[\frac{\partial}{\partial x}\left(K\frac{\partial T}{\partial x}\right)+\frac{\partial}{\partial y}\left(K\frac{\partial T}{\partial y}\right)+\frac{\partial}{\partial z}\left(K\frac{\partial T}{\partial z}\right)\right]+\\&+\left[\frac{\partial}{\partial x}\sum_i(\rho_i h_i V_i)_x+\frac{\partial}{\partial y}\sum_i(\rho_i h_i V_i)_y+\frac{\partial}{\partial z}\sum_i(\rho_i h_i V_i)_z\right]-p\left(\frac{\partial u}{\partial x}+\frac{\partial v}{\partial y}+\frac{\partial w}{\partial z}\right)+\Phi\end{aligned} \tag{5}$$

The first term on the right of eq. (5) is the radiation heat transfer term, the second term is the heat flow term of heat conduction heat transfer, and the third term is the heat exchange term generated by component diffusion, where V_i is the component of the diffusion velocity of component *i* in the *x*-direction, and Φ – the dissipative power.

Mathematical model of combustion

The NO emission forms mainly include the thermal type, prompt type, and fuel type. The fuel used in the small flue gas self-circulation burner studied in this paper was light diesel oil, in which the N content is very low and the generation of fuel NO can be ignored. Therefore, we only considered the generation of thermal-type and prompt-type NO. The generation of thermal NO can be predicted by an extended Zeldovich mechanism:

$$N_2 + O \Leftrightarrow NO + N \text{ (R1)}$$
$$O_2 + N \Leftrightarrow NO + O \text{ (R2)}$$
$$N + OH \Leftrightarrow NO + H \text{ (R3)}$$

The concentration of [O] can be obtained by the local equilibrium method:

$$[\mathrm{O}]=36.64^{0.5}[\mathrm{O_2}]^{0.5}\exp\left(-\frac{27123}{T}\right) \tag{6}$$

The expression of the generation velocity, *v*, of the prompt NO:

$$v_\text{P-NO}=f_\mathrm{c}k_\text{prompt}[\mathrm{O_2}]^\beta[\mathrm{N_2}][\mathrm{C_{12}H_{23}}]\exp\left(-\frac{E}{\mathrm{R}T}\right) \tag{7}$$

where $k_\text{promt} = 6.4\cdot10^6$, E = 72500 cal/gmol, and β is the oxygen response index, which depends on the flame conditions and is only related to the mole fraction of oxygen X_{O2} in the flame. The expression [23]:

$$\beta = \begin{cases} 1.0, & X_{O_2} \le 4.1\cdot 10^{-3} \\ -3.95 - 0.9\ln X_{O_2}, & 4.1\cdot 10^{-3} \le X_{O_2} \le 1.11\cdot 10^{-2} \\ -0.35 - 0.1\ln X_{O_2}, & 1.11\cdot 10^{-2} \le X_{O_2} \le 0.33 \\ 0, & X_{O_2} \ge 0.33 \end{cases} \tag{8}$$

The f_c is the correction coefficient determined by the equivalence ratio and fuel type [24]:

$$f_c = 4.75 + 0.0891n - 23.2\phi + 32\phi^2 - 12.2\phi^3 \tag{9}$$

where n = 12, referring to the number of carbon atoms in the fuel formula and ϕ is the equivalence ratio.

For solving the N-S equation of turbulence, we chose the most basic standard k-ε turbulence model. This model has been verified by numerical calculations of various non-premixed combustors, which can be solved both accurately and quickly. A pressure atomizing model was used to simulate the atomizing process of light oil. After the fuel was atomized, the liquid particles were added by the discrete phase model, for which the Lagrange method was adopted to track the movement and transport of the discrete liquid droplets. In the combustion model, we adopted the non-premix combustion model of the probability density function of the conserved scalar method, which has the advantage that the concentration of each component can be derived by solving the transport equation of one or two conserved scalars (mixed fraction). The fuel components of the light oil used in the small flue gas self-circulation burner could be simplified to $C_{12}H_{13}$, and there were a total of 21 components of all combustion products. In the combustion process, gas radiation has an important influence on the distribution of the atomized combustion temperature field and wall heat transfer, so gas radiation must be considered in the combustion simulation. The DO model namely the discrete ordinates model, is chosen for the radiation model. This model is computationally intensive but can be applied to any medium with optical thickness. It can also consider the radiation heat exchange between gas and particles. The selected mathematical models are listed in tab. 1, which also contains the various boundary conditions.

Table 1. Models and boundary conditions

Model	Detailed settings	Boundary conditions
Turbulence model	Standard k-ε	
Radiation model	DO radiation model	No-slip on the wall: u = 0, v = 0, w = 0 Inner wall emissivity of the combustion chamber: 0.6
The gas-phase combustion model	PDF model with 21 reaction components	Air mass-flow: 0.01138 kg/s, T = 300 K, Outlet pressure: 35 Pa, T = 1200 K;
Discrete phase model	Stochastic tracking method	Light diesel oil ($C_{12}H_{23}$) Mass-flow rate: 0.0001444 kg/s, T = 300 K
Atomization model	Pressure atomization crushing model	Injection pressure P = 1.2 MPa
Pollutant formation models	Extended Zeldovich mechanism prediction [25] and local equilibrium method	Equivalence ratio ϕ = 0.926

Discretization and solution of equations

To ensure the reliability of the calculation results, the convection term was calculated with second-order precision, and the semi-implicit method for pressure linked equations (SIMPLE) algorithm was adopted to solve the coupling of pressure and velocity. In order to speed up the calculation and ensure the convergence of the calculation, the following steps were adopted in the calculation:
– the non-reactive cold air-flow field was calculated to convergence,
– the particle phase was added to solve the equations, except for the radiation and NO models,
– the reaction flow field to be burned was basically stable, and the DO radiation model was added to continue solving until convergence, and
– because the concentration of NO generated in the combustion system is usually low, the NO compound has little impact on the prediction of the flow field, temperature, and concentration of main combustion products.

Thus, in the last step, only the NO generation model and temperature equation were retained, and the distribution of the pollutant field was calculated in the post-treatment.

Mesh independence and model validation

In previous studies on the proportions of the air distribution, we verified the correctness of the numerical model from the aspects of flame height and flame temperature, and we examined the influence of different grid sizes (100.000~380.000 cells) on flame height. The detailed results were presented in the literature [8], and here we will cover only the key results of grid independence and model validation.

The Riello 40G5 type burner was used as the prototype model for experimental verification. This is because the new self-circulation burner structure is an improved design based on this burner, and the basic size is the same. The minimum mesh volume was $1.04 \cdot 10^{-10}$ m^3, and the maximum mesh volume was $1.35 \cdot 10^{-6}$ m^3. The maximum skewness of grids is used as the evaluation standard for grid quality, and its value was 0.74, which meets the requirement of less than 0.85 for good grid quality. Figure 5 shows mesh-independent verification of the flame height and maximum flame temperature on this numerical model.

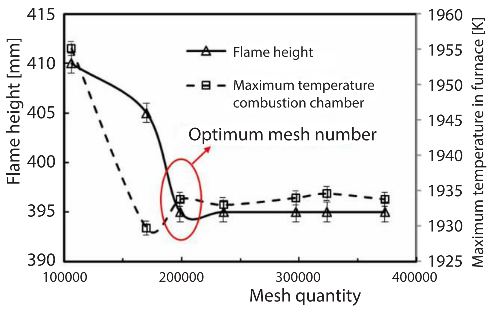

Figure 5. Independence of the present solution from the mesh size: flame height and flame temperature

As the number of grid cells increases, the calculation results tend to be more stable. That is, the maximum temperature of the flame and the height of the flame defined by the average mixing fraction gradually decrease and become stable. Considering the calculation time cost, the minimum number of grid cells that tends to be stable for both the flame height and the maximum flame temperature can be selected as the optimum mesh number for the following numerical calculation. After grid independence verification and calculation cost considerations, 196.000 element mesh models were selected to study the influence of different spray cone angles on the flame.

Results and discussion

Flame height and emissions are two main characteristics of combustion [26, 27]. The spray cone angle mainly affects the distribution of diesel droplets after nozzle exit, and it causes changes in the flame morphology and temperature distribution, which may affect the reversed flow ratio and NO emission characteristics. In the following sections, we analyze the variation rules of the flame temperature field, flame height, and NO emission characteristics. It is important to note that in the simulated experimental conditions, when the spray cone angle was 80° or 90°, the flame morphology was shifted laterally in the radial direction; in particular, when the nozzle cone angle was 90°, the spray droplets in the discrete phase collided with the wall. Because droplets hit the wall at 90°, this spray cone angle is not suitable for engineering applications, so we did not consider this situation in our analysis. The discussion in this chapter is based on numerical calculation results. Although grid independence and prototype burners were verified in the past, this new type of self-circulation flue gas burner has not been tested yet.

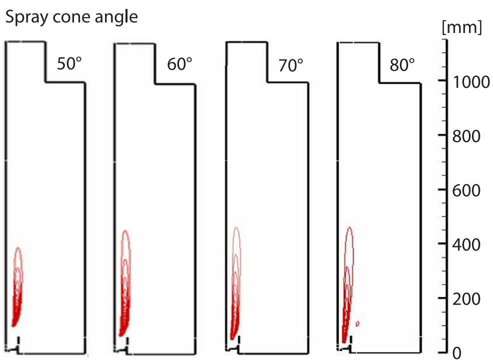

Figure 6. A comparison of the flame morphology under different spray cone angles

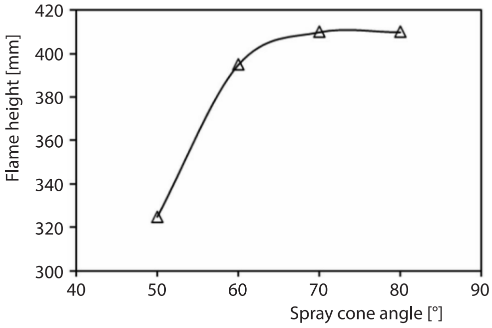

Figure 7. The change curve of flame height dimension with spray cone angle

Flame height

The flame configuration parameter is an important parameter of the flame characteristics [28], especially the flame height. It can be seen from fig. 6 that the flame length is the shortest at a cone angle of 50°. The change in flame height with spray cone angle between 60° and 80° is not very obvious. This is because in the case of 35% central air, 25% swirling air, and 40% secondary air, the central air volume accounts for a large proportion. That is, when the air-flow momentum of the central part is high, the spray cone angle has no significant influence on the flame height.

With increasing spray cone angle, the flame morphology is shifted outwardly in the radial direction. For a spray cone angle of 80°, it is obvious that the maximum flame width is outside the combustion cylinder in the radial direction. When it increases to 90°, the discrete phase spray droplets hit a wall.

Detailed results of the flame height values varying with the spray cone angle are shown in fig. 7. If a shorter flame is needed in practical engineering, a 50° nozzle can be used for the burner, the resulting flame is more than 20% shorter than the flame produced with a 70° spray cone angle. This is inconsistent with the previous conclusion for a high power burner that a smaller spray cone angle makes the flame volume expand and the flame lengthen. The most important reason for this difference is that the self-circulation combustion mode of negative pressure dilutes the oxygen content and preheats the air at the same time. Although the oxygen content in the combustion air decreases, the combustion speed does not decrease but speeds up the fuel combustion, and the flame length becomes shorter as the temperature rises. Second, when the spray cone angle is reduced to 50°, there is less fuel in the secondary air, and the enhanced ejection capacity also shortens the flame.

The NO emissions

The NO emissions are one of the most important properties of the flame, and NO is one of the most representative pollutants. The NO concentration at the exit of the combustion chamber is the best standard to evaluate the final emissions for the whole combustion process. Table 2 shows the variation of the NO concentration at the exit with the spray cone angle. According to China's *General technical requirements for low power oil fuel burners* and the common standards in other parts of the world, we used a 3% reference oxygen concentration as the calculation standard for NO concentration conversion. The oxygen content at the outlet section of the furnace calculated numerically was 1.35%, which was converted to the internationally accepted NO emission concentration for a reference oxygen content of 3%:

$$(\mathrm{NO})_{3\%\mathrm{O}_2} = (\mathrm{NO})_{1.35\%\mathrm{O}_2} \frac{20.9-3.0}{20.9-1.35} \tag{10}$$

Table 2. The concentration of NO emissions at the exit under different spray cone angles

Spray cone angle [°]	NO emission concentration [mgm^{-3}] (1.35% O_2)	NO emission concentration [mgm^{-3}] (3% O_2)
50	22.03	20.17
60	17.33	15.87
70	14.01	12.83
80	10.07	9.22

Under a 3% reference oxygen content, the NO emission concentration of this self-circulation burner is far lower than the NO emission standard for China's fuel burners (200 mg/m^3). Generally speaking, the NO emissions of small flue gas self-circulation burners are relatively low. This is due to the reversed flow of inert combustion products at the opening of the combustion cylinder, which dilutes the chemical reaction zone and reduces the hot spot of the flame at high temperatures. With increasing spray cone angle, the concentration of NO emissions at the exit gradually decreases, and the NO emission at 80° is only about 45% that at 50°, which indicates that the emission reduction effect is obvious. Therefore, although the flame length is shortened at a 50° spray cone angle, the pollutant emission rate is higher, which is related to the reversed flow rate and combustion temperature of the self-circulating flue gas and other factors. We will discuss these in more detail in the next section.

Temperature field and comprehensive analysis

The relationships between flame height, NO emissions, and spray cone angle were analyzed separately. In fact, the spray cone angle affects the distribution characteristics of the initial droplets and, thus, the combustion temperature, while a burner with a flue gas self-circulation structure in turn affects the flow distribution and combustion intensity in the combustion center.

Figure 8 shows the temperature distribution contours on the axial section when the spray cone angle varies from 50-80°. For the axial direction of the *Z*-axis, the temperature of the flame basically increases first and then decreases, because the secondary high temperature area of the flame exists in the middle and front parts of the flame. As a whole, the distribution of flame temperature is similar to that of flame height. With increasing spray cone angle, the overall temperature of the combustion chamber shows a downward trend. This is precisely because most of the NO is thermal, so NO emission at the exit decreases with increasing spray cone angle.

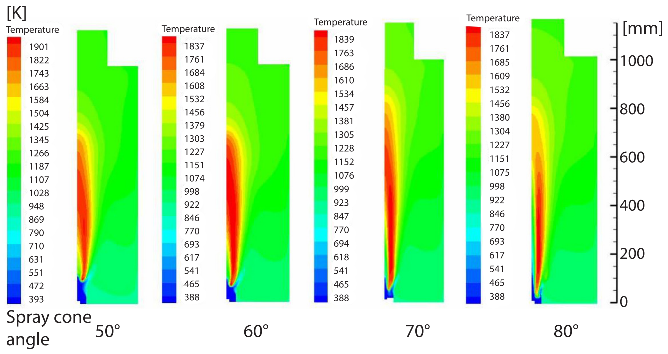

Figure 8. The temperature profiles of the combustion chamber axial section at different spray cone angles

The flue gas re-circulation ratio has an important effect on the initial combustion area of the small flue gas self-circulation burner. Table 3 lists the quantities of reversed-flow flue gas and flue gas self-circulation ratios at different spray cone angles. It can be seen that the flue gas self-circulation rate does not increase monotonically. It first increases with increasing nozzle cone angle, reaches a maximum at 60°, and then decreases accordingly. This is mainly because the size of the spray cone angle directly affects the speed of secondary air and then affects the pressure difference inside and outside the combustion cylinder. However, if the spray cone angle is too large (greater than 60°), the position of the reaction zone moves outward, which also reduces the self-circulation ratio of the flue gas.

Table 3. The relationship between the spray cone angle and re-circulation ratio

Quantity of reversed flow [kgs^{-1}]	Exit mass-flow rate [kgs^{-1}]	Re-circulation ratio [–]
0.0002932	0.002419	12.12
0.0003893	0.002420	16.09
0.0003602	0.002420	14.88
0.0003136	0.002420	12.96

When the spray cone angle is relatively small (from 60-50°), as mentioned in section *Flame height*, the increased combustion speed in the reversed-flow zone and the reduction of fuel in the secondary air lead to flame shortening, and the flue gas reversed flow is correspondingly reduced. As the spray angle continues to increase, the reversed flow of the flue gas self-circulation decreases gradually. This is because when the spray cone angle increases to a certain value, the reaction area near the combustion head moves outwardly and the gas in the reaction area expands with heat, resulting in a decrease in density, meanwhile, the flue gas reversed flow is restricted by volume flow, so the reversed flow quantity decreases accordingly. The fundamental reason for this phenomenon is that the pressure of outward expansion of the gas inside the combustion cylinder increases, so the pressure difference outside the combustion cylinder decreases, resulting in a decrease in the quantity of the backflow.

Conclusions

In this paper, the flame characteristics of a new type of small diesel spray burner with self-circulating flue gas under different spray cone angles (50-90°) were investigated using a periodic model and the CFD. This mainly included investigations of the flame height, temperature distribution, and NO emission characteristics. Our main conclusions are as follows.

- To obtain a shorter flame, a small flue gas self-circulation burner requires a nozzle with a spray cone angle of 50°.
- The NO emissions are still dominated by the thermal type. With an increase of the spray cone angle to 80° and a decrease in the overall combustion temperature, NO emissions are significantly reduced to as low as 9.22 mg/m^3 under 3% O_2 reference flue gas conditions.
- An increase in the spray cone angle leads to a positive gain in the reversed flow ratio from a physical perspective and a negative gain from a chemical combustion perspective. The reversed flow ratio of this small flue gas self-circulation burner reaches its maximum at a 60° spray cone angle.

Acknowledgment

This research was funded by the National Key R&D Program of China under Grant No. 2017YFC0806303 and the Doctor Foundation of Weifang University of Science and Technology under Grant No. KJRC2020004.

Nomenclature

D_i – diffusion coefficient of component *i*
f_c – correction coefficient
f_i – mass force on a unit mass of fluid
k – turbulent kinetic energy
L – flame length, [mm]
m_r – quantity of reversed flow flue gas, [kgs^{-1}]
m_{out} – exit mass-flow rate, [kgs^{-1}]
p – pressure, [Pa]
t_{ij} – viscous stress tensor
T – flame temperature, [K]
u_i – instantaneous velocity in the *i*-direction
v – diffusion velocity
w – formation rate of the net reaction
X – horizontal length above the nozzle, [mm]
Y – concentration of component

Greek symbols

β – oxygen response index
ε – turbulence dissipation rate
η_r – flue gas self-circulation ratio
ρ – density
φ – equivalence ratio
Φ – dissipative power

Subscript

0 – initial state
i – component

References

[1] Xie, K., *et al.*, Experimental Study on Flame Characteristics and Air Entrainment of Diesel Horizontal Spray Burners at Two Different Atmospheric Pressures, *Energy*, *211* (2020), Nov., 118906
[2] Jamrozika, A., *et al.*, Numerical Simulation of Two-Stage Combustion in SI Engine with Prechamber, *Applied Mathematical Modelling*, *37* (2013), 5, pp. 2961-2982
[3] Fan, X., *et al.*, Establishment of Refined Sintering Flue Gas Recirculation Patterns for Gas Pollutant Reduction and Waste Heat Recycling, *Journal of Cleaner Production*, *235* (2019), Oct., pp. 1549-1558
[4] Dally, B., *et al*., Effect of Fuel Mixture on Moderate and Intense Low Oxygen Dilution Combustion, *Combustion and Flame*, *137* (2004), 4, pp. 418-431
[5] Zeng, G., *et al*., Influences of Initial Coal Concentration on Ignition Behaviors of Low-NO_x Bias Combustion Technology, *Applied Energy*, *278* (2020), Nov., 115745
[6] Mancini, M., *et al*., On Mathematical Modelling of Flameless Combustion, *Combustion and Flame*, *150* (2007), 1, pp. 54-59
[7] Shinomori, K., *et al*., NO_x Emission Characteristics and Aerodynamic Structure of a Self-Recirculation Type Burner for Small Boilers, *Proceedings of the Combustion Institute*, *33* (2011), 2, pp. 2735-2742

[8] Xie, K., *et al*., Effect of Air Quantity Distribution Ratio on Flame Height of Flue Gas Self-Circulation Burner, *Journal of Applied Fluid Mechanics*, *13* (2020), 1, pp. 233-243
[9] Xu, Q., *et al*., Performance Analysis of Novel Flue Gas Self-Circulated Burner Based on Low-NO_x Combustion, *Journal of Energy Engineering*, *146* (2020), 2, 04019041
[10] Xu, Q., *et a*l., Effects of Optimized Operating Parameters on Combustion Characteristics and NO_x Emissions of a Burner based on Orthogonal Analysis, *Journal of Thermal Science*, *30* (2020), July, pp. 1212-1223
[11] Jones, W. P., *et al*., An Investigation of a Turbulent Spray Flame Using Large Eddy Simulation with a Stochastic Breakup Model, *Combustion and Flame*, *186* (2017), Dec., pp. 277-298
[12] Datta, A., Som, S. K., Numerical Prediction of Air Core Diameter, Coefficient of Discharge and Spray Cone Angle of a Swirl Spray Pressure Nozzle, *International Journal of Heat and Fluid Flow*, *21* (2000), 4, pp. 412-419
[13] Huang, Y., *et al*., Effect of Liquid Viscosity and Swirl Chamber Length on the Air Core And Spray Cone Angle From Pressure-Swirl Atomizers, *Proceedings*, International Conference on Energy and Mechanical Engineering, Hong Kong, China, 2015, pp. 642-650
[14] Sharma, S., *et al*., On the Effect of Spray Parameters on CO and NO_x Emissions in a Liquid Fuel Fired Flameless Combustor, *Fuel*, *199* (2017), Jul., pp. 229-238
[15] Yang, S. I., *et al*., Spray Combustion Characteristics of Kerosene/Bio-Oil – Part I: Experimental Study, *Energy*, *119* (2017), Jan., pp. 26-36
[16] Vengatesh, P., *et al*., Spray Characteristics of Diesel Fuel Using Numerical Simulation, *International Research Journal of Engineering and Technology*, *5* (2018), 4, pp. 1074-1077
[17] Bonefačić I., *et al*., Improvement of Fuel Oil Spray Combustion Inside a 7 MW Industrial Furnace: A Numerical Study, *Applied Thermal Engineering*, *110* (2017), Jan., pp. 795-804
[18] San Jose, J., *et al*., Spray Characteristics, Combustion Performance, and Palm Oil Emissions in a Low-Pressure Auxiliary Air Fluid Pulverization Burner, *Energy & Fuels*, *32* (2018), 11, pp. 11502-11510
[19] Amoresano, A., *et al*., Experimental Characterization of a Pressure Swirl Spray by Analyzing the Half Cone Angle Fluctuation, Experimental Thermal and Fluid Science, *94* (2018), June, pp. 122-133
[20] Dikshit, S. B., *et al*., Factors Affecting Spray Cone Angle of Pressure Swirl Atomizer for Gas Turbine Combustion Chamber: Theoretical and Experimental Analysis, *Indian Journal of Science and Technology*, *11* (2018), 8, pp. 1-4
[21] Xie, K., *et al*., Experimental Study on the Effect of Spray Cone Angle on the Characteristics of Horizontal Jet Spray Flame under sub-Atmospheric Pressure, *Thermal Science*, *24* (2020), 5A, pp. 2941-2952
[22] Umyshev, D. R., *et al*., Experimental Investigation of V-Gutter Flameholders, *Thermal Science*, *21* (2017), 2, pp. 1011-1019
[23] DeSoete, G., Overall Reaction Rates of NO and N_2 Formation from Fuel Nitrogen, *Symposium (International) on Combustion*, *15* (1975), 1, pp. 1093-1102
[24] Bachmaier, F., *et al*., The Formation of Nitric Oxide and the Detection of HCN in Premixed Hydrocarbon-Air flames at 1 Atmosphere, *Combustion Science and Technology*, *7* (1973), 2, pp. 77-84
[25] Anetor, L., *et al*., Computational Analysis of the Extended Zeldovich Mechanism, Arabian Journal for Science and Engineering, *39* (2014), 11, pp. 8287-8305
[26] Jovanović, R. D., *et al*., Experimental and Numerical Investigation of Flame Characteristics during Swirl Burner Operation under Conventional and Oxy-Fuel Conditions, *Thermal Science*, *21* (2017), 3, pp. 1463-1477
[27] Zhang, N., *et al*., On the Laminar Combustion Characteristics of Natural Gas-Syngas-Air Mixtures, *Thermal Science*, *22* (2018), 5, pp. 2077-2086
[28] Javareshkian, A., *et al*., An Experimental Study on the Effects of Swirling Oxidizer Flow and Diameter of Fuel Nozzle on Behaviour and Light Emittance of Propane-Oxygen Non-Premixed Flame, *Thermal Science*, *21* (2017), 3, pp. 1453-1462

Paper submitted: December 29, 2020
Paper revised: February 3, 2021
Paper accepted: February 10, 2021